

Generation of the Maxwellian inflow distribution

Alejandro L. Garcia ^{a,*}, Wolfgang Wagner ^b

^a Department of Physics, San Jose State University, Science Building, Room 245, One Washington Square, San Jose, CA 95192-0106, USA

^b Weierstrass Institute for Applied Analysis and Stochastics, Mohrenstrasse 39, 10117 Berlin, Germany

Received 23 February 2005; received in revised form 11 January 2006; accepted 17 January 2006
Available online 3 March 2006

Abstract

This paper presents several efficient, exact acceptance–rejection methods for generating the Maxwellian inflow distribution, the velocity distribution of gas molecules crossing a plane. The new methods are demonstrated to be computationally faster and more accurate than the schemes commonly used for open boundary conditions in particle simulations.

© 2006 Elsevier Inc. All rights reserved.

Keywords: Random number generation; Direct simulation Monte Carlo; Open boundary conditions; Acceptance–rejection methods

1. Introduction

Stochastic algorithms, commonly referred to as Monte Carlo methods, use random numbers generated from a variety of distributions. Efficient generators have been developed for the most commonly used distributions (e.g., uniform, Gaussian, and exponential) and general techniques (e.g., inversion) are available for arbitrary distributions [1,2]. However, generating a complicated distribution by a generic method may not be efficient or accurate, which is why specialized generators for specific applications are welcome.

This paper discusses the generation of random values z from the distribution

$$p_a(z) = \frac{2(a-z)\exp(-z^2)}{\exp(-a^2) + a\sqrt{\pi}[1 + \operatorname{erf}(a)]}, \quad z < a, \quad (1.1)$$

where a is some real-valued parameter and erf denotes the error function (cf. (A.12)). As shown in Sections 2 and 3, this distribution arises when implementing the inflow boundary condition for particles crossing a surface. Specifically, it is associated with the velocity distribution of particles, Maxwellian distributed in their moving frame of reference, that pass through a plane. This boundary condition is very common in molecular simulations of hydrodynamic flows in open systems [3,4]. With this association, we call $p_a(z)$ the Maxwellian inflow distribution. Note that for $a = 0$ the distribution (1.1) reduces to the Rayleigh distribution, which is trivial to generate [1].

* Corresponding author. Tel.: +1 408 924 5244; fax: +1 408 924 4815.
E-mail address: algarcia@algarcia.org (A.L. Garcia).

Section 3 describes the general algorithm for generating the random velocities of particles for an inflow boundary condition. For the Maxwellian inflow distribution (1.1) there are three methods for random variate generation that are in common use. The first is inversion (see Section 4), which has the disadvantage of being computationally expensive. The other two are approximate acceptance–rejection schemes, discussed in [5] and in Section 5.1, which are more efficient than inversion but not exact.

In Section 5.2, we develop several *exact* acceptance–rejection schemes that are more efficient than any of the three methods in common use. The computational efficiency of all the schemes is discussed in Section 6. Their programming implementation in a practical example is summarized in Section 7. We conclude in Section 8 with some further remarks regarding applications of the present schemes and their extension to other distributions.

2. Maxwellian inflow

This section establishes the mathematical formulation for inflow boundary conditions. Readers interested in a more physical introduction, presented in the context of a specific example, are directed to Section 7.

The general inflow boundary condition for the Boltzmann equation [6] is

$$f(t, x, v)(v, n(x)) = b(x, v),$$

where $t \geq 0$, $x \in \partial D$ and the velocity $v \in \mathcal{R}^3$ is such that $(v, n(x)) > 0$. Here, ∂D denotes the boundary of the spatial domain D ; $n(x)$ is the unit inward normal vector at $x \in \partial D$; (v, n) is the scalar (dot) product of vectors v and n . The function b determines the inflow intensity (waiting time parameter)

$$\lambda = \frac{1}{g} \int_{\partial D} \int_{(v, n(x)) > 0} b(x, v) dv \sigma(dx) \tag{2.1}$$

and the inflow law

$$\frac{1}{g\lambda} b(x, v), \tag{2.2}$$

where $\sigma(dx)$ denotes the uniform surface measure (area) on ∂D and g is the weight of the incoming particles. A case of special interest is Maxwellian inflow

$$b(x, v) = \begin{cases} M_{\varrho, V, T}(v)(v, e) & \text{if } x \in \Gamma, \quad (v, e) > 0, \\ 0 & \text{otherwise,} \end{cases}$$

where

$$M_{\varrho, V, T}(v) = \frac{\varrho}{(2\pi T)^{3/2}} \exp\left(-\frac{\|v - V\|^2}{2T}\right)$$

is the Maxwellian distribution and

$$e = n(x) \quad \forall x \in \Gamma \subset \partial D,$$

is the unit normal for some plane part Γ of the boundary. The inflow intensity (2.1) takes the form

$$\lambda = \frac{1}{g} \sigma(\Gamma) C, \tag{2.3}$$

where

$$C = \int_{(v, e) > 0} M_{\varrho, V, T}(v)(v, e) dv. \tag{2.4}$$

According to the inflow law (2.2), the position of the incoming particle is distributed uniformly on Γ , the inflow boundary, and the particle enters the domain by leaving this boundary at a random time [5,7,8]. Its velocity is generated according to the probability density

$$q(v) = \begin{cases} C^{-1}M_{\varrho,V,T}(v)(v, e) & \text{if } (v, e) > 0, \\ 0 & \text{otherwise.} \end{cases} \tag{2.5}$$

3. General algorithm

We now turn to the question of how to generate a random variable ξ according to the probability density (2.5). Employing a standard substitution, which for completeness is presented in Appendix A, the problem is reduced to generating from the density

$$\tilde{q}(w_1, w_2, w_3) = \begin{cases} 2m(a)^{-1}\pi^{-1}(a + w_3) \exp(-\|w\|^2) & \text{if } a + w_3 > 0, \\ 0 & \text{otherwise,} \end{cases}$$

where

$$a = \frac{(V, e)}{\sqrt{2T}} \tag{3.1}$$

is the speed ratio and

$$m(x) = \exp(-x^2) + x\sqrt{\pi}[1 + \operatorname{erf}(x)], \quad x \in \mathcal{R}. \tag{3.2}$$

The components of w are independent; the first two components are distributed according to the probability density

$$\frac{1}{\pi} \exp(-w_1^2 - w_2^2), \quad w_1, w_2 \in \mathcal{R},$$

and the third is obtained as

$$w_3 = -z, \tag{3.3}$$

where z is distributed according to the Maxwell inflow distribution

$$p_a(z) = \frac{2}{m(a)}(a - z) \exp(-z^2), \quad z \in (-\infty, a). \tag{3.4}$$

The random variable ξ is obtained as (cf. (A.2), (3.3))

$$\xi = V + \sqrt{2T}Q(e) \begin{pmatrix} w_1^* \\ w_2^* \\ -z^* \end{pmatrix}, \tag{3.5}$$

where Q is a coordinate rotation matrix (cf. (A.1)). The variables w_1^* and w_2^* are independent Gaussians with zero mean and variance 1/2. In the case $a = 0$, one obtains from the inverse transformation (see Section 4) and (A.10)

$$z^* = -\sqrt{-\log u}, \tag{3.6}$$

where u is uniformly distributed on (0, 1). The generation of the variable z^* in the case $a \neq 0$, which is the point of this paper, will be discussed in the following sections.

4. Inverse transform

One method to obtain the component z^* to be used in (3.5) is by the inverse transform method [1,2], that is, by solving numerically the equation

$$\int_{-\infty}^z p_a(x) dx = u, \quad z < a, \tag{4.1}$$

where u is uniformly distributed on $(0, 1)$. Denote the left-hand side of Eq. (4.1) by $F_a(z)$. According to (A.9) (A.10), and (3.4), one obtains

$$F_a(z) = \frac{1}{m(a)} \{ \exp(-z^2) + a\sqrt{\pi}[1 + \operatorname{erf}(z)] \}.$$

Furthermore, $F'_a(x) = p_a(x)$ and

$$p'_a(z) = \frac{2}{m(a)} \exp(-z^2)[2z^2 - 2za - 1].$$

Thus, the function F_a has an inflection point at

$$z(a) = \frac{a - \sqrt{a^2 + 2}}{2}, \tag{4.2}$$

and the function p_a takes its maximum there, that is,

$$\max_{z < a} p_a(z) = p_a(z(a)). \tag{4.3}$$

Note that $z(a) < \min(a, 0)$.

Eq. (4.1) is solved by a Newton iteration, starting with the initial guess $z_0 = z(a)$. Calculate the error

$$E_k = F_a(z_k) - u, \quad k = 0, 1, 2, \dots,$$

and stop if it is small enough, specifically if $|E_k| < E_d$. Otherwise, calculate the new guess

$$z_{k+1} = z_k - \frac{E_k}{F'_a(z_k)} = z_k - \frac{m(a)E_k}{2(a - z_k) \exp(-z_k^2)}$$

and continue the iteration.

The inversion method, as described above, has the disadvantage of being computationally expensive relative to other generators, as discussed in Section 6. An alternative to Newton iteration is to pre-compute $F_a(z)$, use (4.1) to tabulate $F_a^{-1}(u)$ and then generate z by interpolated table lookup. For the Maxwellian inflow distribution there are several disadvantages to this approach: First, the infinite tail of the distribution must be treated separately, typically by acceptance–rejection (see the following section). Second, the scheme is not exact and a large table, costing computer memory, with a good interpolation scheme, costing computer time, are needed to maintain accuracy. Finally, the table of F_a^{-1} must be recomputed for each different value of a . Given the computational efficiency of the generators presented in this paper (see Section 6) it is unlikely that inversion by table lookup, or other table methods [1], would be competitive.

5. Acceptance–rejection

This section discusses the use of the acceptance–rejection technique to generate the component z^* to be used in (3.5). This technique is based on selecting a suitable majorant (envelope) \hat{p} such that (cf. (3.4))

$$p_a(z) \leq \hat{p}(z) \quad \forall z < a. \tag{5.1}$$

The component z^* is generated according to the probability density

$$\frac{1}{\int_{-\infty}^a \hat{p}(x) dx} \hat{p}(z), \quad z < a, \tag{5.2}$$

and is accepted with probability

$$\frac{p_a(z^*)}{\hat{p}(z^*)} \tag{5.3}$$

so

$$\frac{1}{\int_{-\infty}^a \hat{p}(x) dx} \tag{5.4}$$

is the acceptance rate.

The efficiency of the acceptance–rejection method obviously depends on the choice of the envelope function \hat{p} . Ideally, the acceptance rate will be close to one and the probability density (5.2) is a distribution that can be generated efficiently.

5.1. Approximate envelopes

This section presents two approximate acceptance–rejection methods that are in common use [5]. The schemes are approximate because the envelopes do not satisfy (5.1) and thus the distributions they generate only approximate $p_a(z)$.

5.1.1. Box envelope

The first approximate method uses a rectangular box envelope (cf. (4.2), (4.3))

$$\hat{p}_B(z) = \begin{cases} p_a(z(a)), & z_{<}(a) < z < z_{>}(a), \\ 0 & \text{otherwise,} \end{cases}$$

where $z_{<}(a) < z_{>}(a) \leq a$ are some parameters to be specified later. Note that

$$\int_{-\infty}^z \hat{p}_B(x) dx = \begin{cases} 0, & z < z_{<}(a), \\ p_a(z(a))(z - z_{<}(a)), & z_{<}(a) < z < z_{>}(a), \\ p_a(z(a))(z_{>}(a) - z_{<}(a)), & z > z_{>}(a). \end{cases}$$

One generates z^* as

$$z^* = z_{<}(a) + (z_{>}(a) - z_{<}(a))u$$

which is accepted with probability (cf. (5.3))

$$\frac{p_a(z^*)}{p_a(z(a))} = \frac{a - z^*}{a - z(a)} \exp(z(a)^2 - (z^*)^2).$$

This method is approximate since the condition (cf. (5.1))

$$p_a(z) \leq \hat{p}_B(z)$$

is not satisfied for $z < z_{<}(a)$ and for $z > z_{>}(a)$. The actual distribution generated by the box envelope is

$$\tilde{p}_a(z) = \begin{cases} p_a(z)/m_B(a), & z_{<}(a) < z < z_{>}(a), \\ 0 & \text{otherwise,} \end{cases}$$

where

$$m_B(a) = \int_{z_{<}}^{z_{>}} p_a(z) dz.$$

5.1.2. Reservoir envelope

The second approximate method uses the envelope

$$\hat{p}_R(z) = \frac{2}{m(a)} (a - z_{<}(a)) \exp(-z^2),$$

where $z_{<}(a) < a$ is some parameter to be specified later. One generates z^* according to the probability density

$$\frac{1}{\sqrt{\pi}} \exp(-z^2) \tag{5.5}$$

so that z^* is a Gaussian with zero mean and variance $1/2$. The generated value is rejected if $z^* > a$, accepted with probability (cf. (5.3))

$$\frac{p_a(z^*)}{\hat{p}_R(z^*)} = \frac{a - z^*}{a - z_{<}(a)} \tag{5.6}$$

if $z^* > z_{<}(a)$, and accepted with probability one otherwise.

The reservoir method is so named because it has the following physical interpretation: A particle is generated in a reservoir with position x and velocity v . The position is chosen uniformly from the interval $(-L, 0)$ and the velocity chosen as $v = a - z$ where z is distributed as (5.5). The particle is accepted if it moves past the origin during a time interval τ , that is,

$$x + v\tau > 0 \quad \text{or} \quad (a - z)\tau > uL.$$

Taking

$$\tau = \frac{L}{a - z_{<}(a)}$$

gives us that z is accepted with probability (5.6).

Note that this method is approximate since the condition (cf. (5.1))

$$p_a(z) \leq \hat{p}_R(z)$$

is not satisfied for $z < z_{<}(a)$. The actual distribution generated by the reservoir envelope is

$$\tilde{p}_a(z) = \frac{1}{m_R(a)} \begin{cases} p_a(z), & z_{<}(a) < z < a, \\ \hat{p}_R(z) & \text{otherwise,} \end{cases}$$

where

$$m_R(a) = \int_{z_{<}}^a p_a(z) dz + \int_{-\infty}^{z_{<}} \hat{p}_R(z) dz.$$

5.1.3. Truncation errors

The error in these approximate methods is most easily seen from the absolute fractional error in the moments, that is,

$$\left| \frac{\langle z^i \rangle - \langle \tilde{z}^i \rangle}{\langle z^i \rangle} \right|,$$

where

$$\langle z^i \rangle = \int_{-\infty}^a z^i p_a(z) dz \quad \text{and} \quad \langle \tilde{z}^i \rangle = \int_{-\infty}^a z^i \tilde{p}_a(z) dz.$$

This error is shown in Fig. 1 for the box and reservoir envelopes using typical values for the parameters (see [5,7]) in these approximate envelopes. For the higher moments, the error is large (a few percent) when $a < 0$. This error can be reduced by suitable choice of the envelopes' parameters but at the price of computational efficiency (see Section 6).

5.2. Exact envelopes

This section presents the main results of this paper, namely, four exact envelope functions, two for each case of negative and positive speed ratio ($a < 0$ and $a > 0$). We later show (see Section 6) that these envelopes yield efficient acceptance–rejection schemes for the Maxwellian inflow distribution. Of the four envelopes presented in this section, the first and the third are most efficient for low-speed ratio ($|a| < \frac{1}{2}$) while the other two are efficient for a broad range of a .

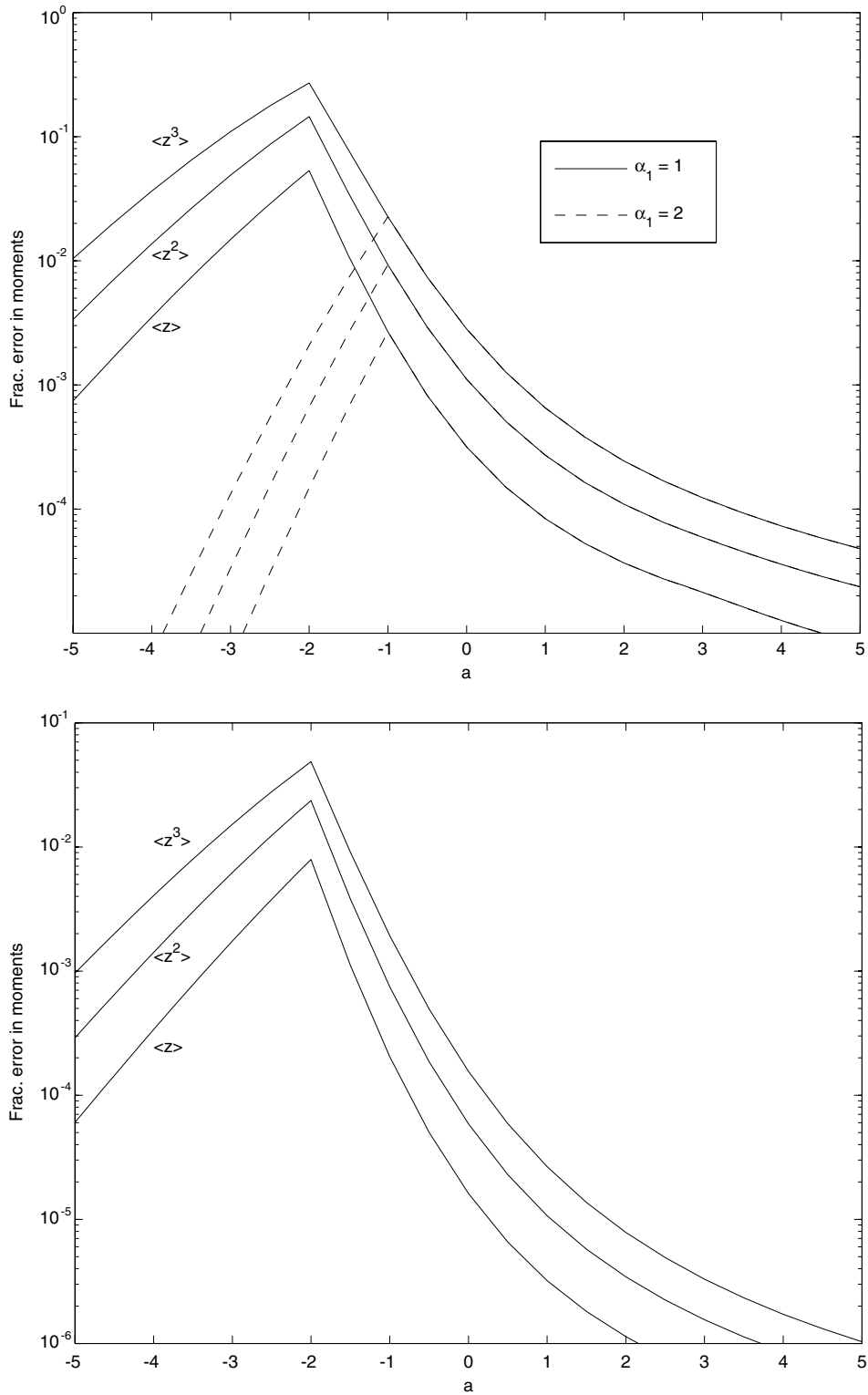


Fig. 1. Absolute fractional error in the first three moments as a function of speed ratio, a . Upper figure is for the box envelope with $z_-(a) = \min(a - \alpha_1, -3)$, $z_+(a) = \min(a, 3)$ for $\alpha_1 = 1$ (solid line) and $\alpha_1 = 2$ (dashed line). Lower figure is the reservoir envelope with $z_-(a) = \min(a - 1, -3)$.

5.2.1. Envelope 1 ($a < 0$)

For $a < 0$, consider the envelope

$$\hat{p}_1(z) = \frac{2}{m(a)}(-z) \exp(-z^2)$$

and note that (cf. (A.10))

$$\int_{-\infty}^z \hat{p}_1(x) dx = \frac{1}{m(a)} \exp(-z^2). \tag{5.7}$$

The acceptance rate (5.4) is

$$\frac{m(a)}{\exp(-a^2)}$$

and tends to 1 as $a \rightarrow 0$ (see Fig. 2). One obtains from (5.7)

$$z^* = -\sqrt{a^2 - \log u} \tag{5.8}$$

and the acceptance probability (5.3) is

$$\frac{a - z^*}{-z^*} \rightarrow \begin{cases} 0 & \text{if } z^* \rightarrow a, \\ 1 & \text{if } z^* \rightarrow -\infty. \end{cases}$$

5.2.2. Envelope 2 ($a < 0$)

For $a < 0$, consider the envelope (cf. (4.2), (4.3))

$$\hat{p}_2(z) = \begin{cases} \hat{p}_1(z) & \text{if } z < \beta(a), \\ p_a(z(a)) & \text{if } z \in [\beta(a), a), \end{cases}$$

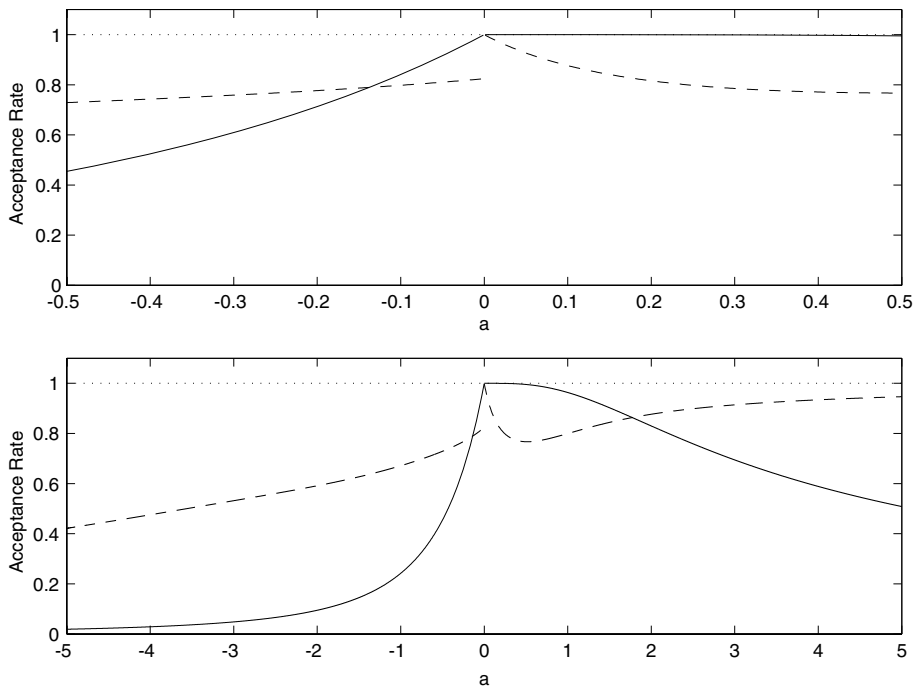


Fig. 2. Acceptance rates for: Envelope 1 (solid line, $a < 0$); Envelope 2 (dashed line, $a < 0$); Envelope 3 (solid line, $a > 0$); Envelope 4 (dashed line, $a > 0$).

where the function β satisfies

$$\beta(a) \leq a.$$

The previous case is obtained for $\beta(a) = a$. One obtains

$$\int_{-\infty}^a \hat{p}_2(z) dz = \frac{1}{m(a)} [\exp(-\beta(a)^2) + 2 \exp(-z(a)^2)(a - z(a))[a - \beta(a)]]$$

and the corresponding acceptance rate (5.4). Our particular choice is

$$\beta(a) = a - (1 - a)(a - z(a)),$$

which gives a favorable acceptance rate over a wide range of a (see Fig. 2).

For this piece-wise envelope, with probability

$$\frac{\exp(-\beta(a)^2)}{\exp(-\beta(a)^2) + 2 \exp(-z(a)^2)(a - z(a))[a - \beta(a)]},$$

z^* is generated according to the probability density

$$2 \exp(\beta(a)^2)(-z) \exp(-z^2), \quad z < \beta(a),$$

so that (cf. (5.8))

$$z^* = -\sqrt{\beta(a)^2 - \log u},$$

and accepted with probability

$$\frac{a - z^*}{-z^*}.$$

With probability

$$\frac{2 \exp(-z(a)^2)(a - z(a))[a - \beta(a)]}{\exp(-\beta(a)^2) + 2 \exp(-z(a)^2)(a - z(a))[a - \beta(a)]}$$

z^* is generated uniformly on $[\beta(a), a]$ and accepted with probability

$$\frac{a - z^*}{a - z(a)} \exp(z(a)^2 - (z^*)^2).$$

5.2.3. Envelope 3 ($a > 0$)

For $a > 0$, consider the envelope

$$\hat{p}_3(z) = \begin{cases} p_a(z) & \text{if } z \leq 0, \\ 2m(a)^{-1}(a - z) & \text{if } z \in (0, a), \end{cases}$$

and note that (cf. (A.9) and (A.10))

$$\int_{-\infty}^a \hat{p}_3(z) dz = \frac{1}{m(a)} (a\sqrt{\pi} + 1 + a^2).$$

The acceptance rate (5.4) is

$$\frac{m(a)}{a\sqrt{\pi} + 1 + a^2},$$

which is shown in Fig. 2 to be close to unity for $a < 1$.

With probability

$$\frac{a\sqrt{\pi}}{a\sqrt{\pi} + 1 + a^2}$$

one generates z^* according to the probability density

$$\frac{2}{\sqrt{\pi}} \exp(-z^2), \quad z \leq 0,$$

so that z^* is a one-sided Gaussian with parameters 0 and 1/2. With probability

$$\frac{1}{a\sqrt{\pi} + 1 + a^2}$$

one generates z^* according to the probability density

$$2(-z) \exp(-z^2), \quad z \leq 0,$$

so that z^* is defined in (3.6). With probability

$$\frac{a^2}{a\sqrt{\pi} + 1 + a^2}$$

one generates z^* according to the probability density

$$\frac{2}{a^2}(a - z), \quad z \in (0, a),$$

so that

$$z^* = a(1 - \sqrt{u}),$$

and accepts it with probability

$$\exp(-(z^*)^2).$$

5.2.4. Envelope 4 ($a > 0$)

For $a > 0$, consider the envelope

$$\hat{p}_4(z) = \begin{cases} p_a(z) & \text{if } z \leq 0, \\ 2m(a)^{-1}a \exp(-z^2) & \text{if } z > 0, \end{cases}$$

and note that (cf. (A.10))

$$\int_{-\infty}^a \hat{p}_4(z) dz = \frac{1}{m(a)} (2a\sqrt{\pi} + 1).$$

The acceptance rate (5.4) is

$$\frac{m(a)}{2a\sqrt{\pi} + 1},$$

which is shown in Fig. 2 to be favorable over a wide range of values, going to unity as $a \rightarrow \infty$.

With probability

$$\frac{2a\sqrt{\pi}}{2a\sqrt{\pi} + 1}$$

one generates z^* according to the probability density

$$\frac{1}{\sqrt{\pi}} \exp(-z^2), \quad z \in \mathcal{R},$$

so that z^* is Gaussian with zero mean and variance 1/2. With probability

$$\frac{1}{2a\sqrt{\pi} + 1}$$

one generates z^* according to the probability density

$$2(-z) \exp(-z^2), \quad z \leq 0,$$

so that z^* is defined in (3.6), and accepts it with probability

$$\frac{p_a(z^*)}{\hat{p}_4(z^*)} = \begin{cases} 1 & \text{if } z^* \leq 0, \\ 1 - z^*/a & \text{if } z^* \in (0, a), \\ 0 & \text{if } z^* \geq a. \end{cases}$$

6. Computational efficiency

The computational efficiencies of the different generators were evaluated by measuring CPU time.¹ Following [5], the relative efficiency was obtained by normalizing these CPU times relative to the CPU time of the box envelope method (see Section 5.1.1) for $a = 0$. Parameter values typical of common usage were used, specifically: $E_d = 10^{-5}$ for inversion; $z_<(a), z_>(a)$ for box and reservoir envelopes, as in Fig. 1. The Merenne twister method [16] and the polar Box-Muller method [10] were used to generate uniformly distributed and normal (Gaussian) distributed random numbers, respectively.

Figs. 3 and 4 present the computational efficiencies of the various methods. The absolute computational expense may be estimated from the observation that, for the case $a = 0$, the generator based on Envelope 1 is only slightly more expensive than generating a pair of uniformly distributed random variables.

Fig. 3 shows that a generator that combines Envelopes 1 and 3 (see Sections 5.2.1, 5.2.3 and Table 1) is the most efficient for low-speed flows ($|a| \ll 1$). Fig. 4 illustrates that a generator based on Envelopes 2 and 4 (see Sections 5.2.2, 5.2.4 and Table 2) is efficient over a wide range of speed ratio.

Inversion is computationally expensive, even though Newton’s method converges quickly and our implementation uses an efficient polynomial approximation for the error function [10]. For $a < -1$ the box method is efficient when $\alpha_1 = 1$ but not accurate (see Fig. 1); for $\alpha_1 = 2$ the box method is not competitive. The reservoir method is very inefficient for $a < 0$ and not competitive with the method using Envelopes 2 and 4 for $a > 0$.

7. Practical example

For the convenience of readers wishing to implement the generators described in this paper this self-contained section illustrates their use in the context of a typical physics application.

Consider particles (mass μ) uniformly distributed in space, with number density ϱ , and Maxwell-Boltzmann distributed in velocity, with mean velocity $\mathbf{V} = (V_x, V_y, V_z)$ and temperature T . The probability distribution for the velocity of particles, $\mathbf{v} = (v_x, v_y, v_z)$, crossing the $y - z$ plane in the $+x$ -direction is

$$p(\mathbf{v}) = C^{-1} v_x \exp(-|\mathbf{v} - \mathbf{V}|^2/v_T^2), \quad v_x > 0,$$

where $v_T = \sqrt{2kT/\mu}$ is the most probable thermal speed, k is Boltzmann’s constant, and C is the normalization constant.

From the inflow intensity (cf. (2.3), (2.4) and (A.13)) the mean number of particles crossing a surface area σ during a time interval τ is

$$\varrho\sigma\tau \frac{v_T}{2\sqrt{\pi}} \{ \exp(-a^2) + a\sqrt{\pi}[1 + \operatorname{erf}(a)] \},$$

where $a = V_x/v_T$ is the speed ratio. Typically an open boundary condition is implemented by determining the number of particles that cross a surface during a time interval and generating those particles at random times, uniformly distributed in the time interval [5,7]. As shown in [9], the random integer number of particles should be chosen from a Poisson distribution with the appropriate mean to avoid anomalous correlations.

¹ The programs used Microsoft Visual C++ and were run on an Intel Pentium M processor.

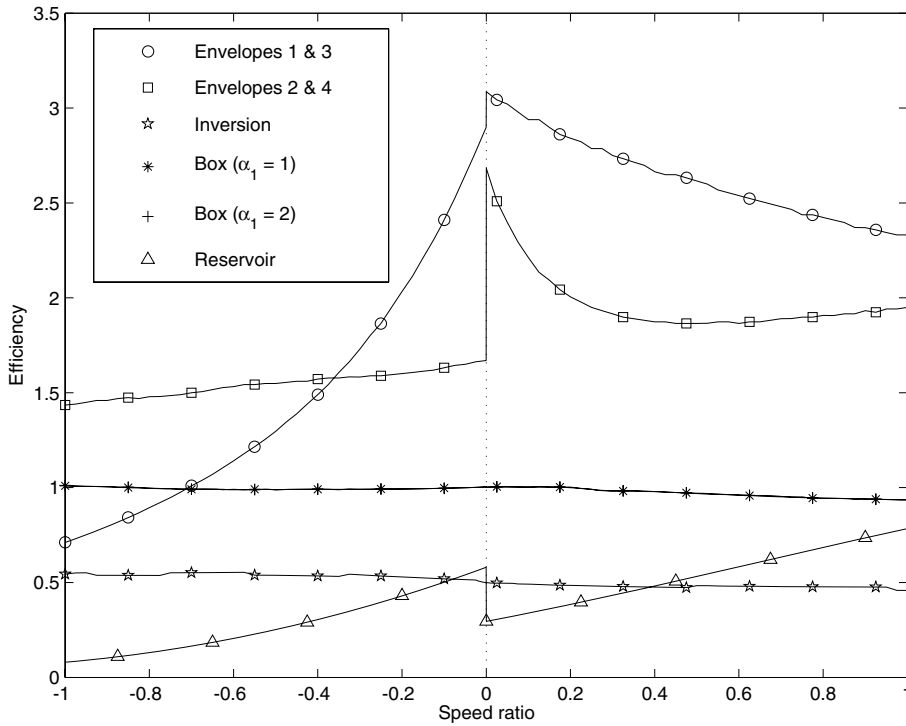


Fig. 3. Relative computational efficiency versus speed ratio in the low-speed ($|a| < 1$) regime. See Fig. 4 caption for legend.

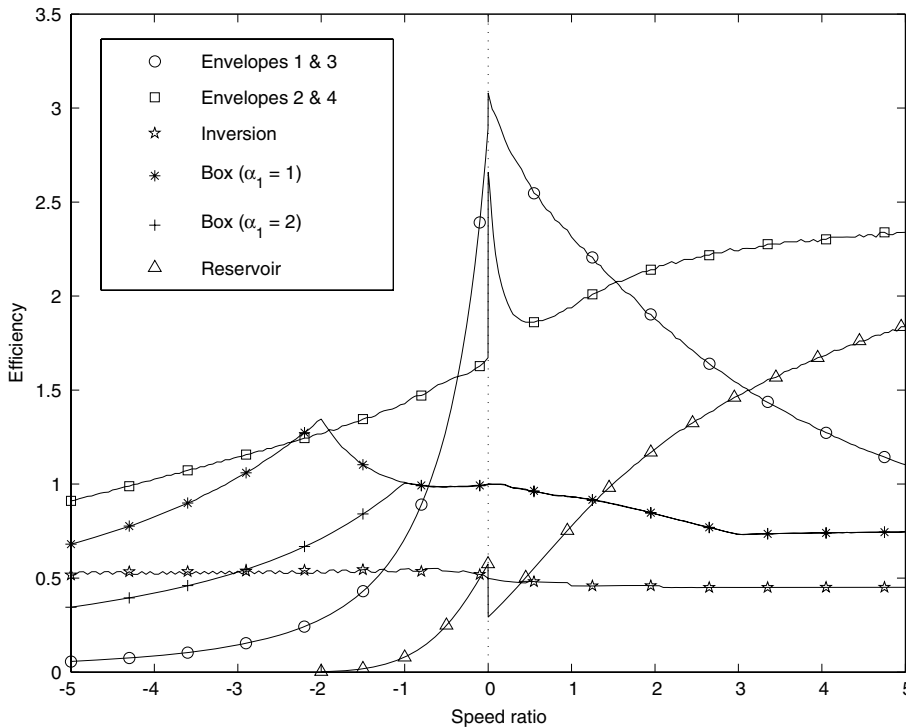


Fig. 4. Relative computational efficiency versus speed ratio. Data is for: Envelopes 1 and 3 (circles); Envelopes 2 and 4 (squares); inversion (stars), box envelope (asterisks for $\alpha_1 = 1$, crosses for $\alpha_1 = 2$), reservoir envelope (triangles).

Table 1
Outline of acceptance rejection method using Envelopes 1 and 3

- If $a \leq 0$,
 1. Compute $z^* = -\sqrt{a^2 - \log \mathfrak{R}_u}$
 2. If $\frac{a-z^*}{-z^*} > \mathfrak{R}'_u$ return z^* , else go to step 1
- If $a > 0$,
 1. Set $u = \mathfrak{R}_u$
 2. If $\frac{a\sqrt{\pi}}{a\sqrt{\pi} + 1 + a^2} > u$ then return $z^* = -\frac{1}{\sqrt{2}}|\mathfrak{R}_u|$
 3. Else if $\frac{a\sqrt{\pi} + 1}{a\sqrt{\pi} + 1 + a^2} > u$ then return $z^* = -\sqrt{-\log \mathfrak{R}'_u}$
 4. Else,
 - (a) Compute $z^* = (1 - \sqrt{\mathfrak{R}'_u})a$
 - (b) If $\exp(-(z^*)^2) > \mathfrak{R}''_u$ then return z^* , else go to step 1

Recommended generator for low-speed problems.

Table 2
Outline of acceptance rejection method using Envelopes 2 and 4

- If $a < 0$,
 1. Set $z(a) = \frac{1}{2}(a - \sqrt{a^2 + 2})$ and $\beta(a) = a - (1 - a)[a - z(a)]$
 2. If, $\frac{\exp(-\beta(a)^2)}{\exp(-\beta(a)^2) + 2[a - z(a)][a - \beta(a)]\exp(-z(a)^2)} > \mathfrak{R}_u$
 - (a) Compute $z^* = -\sqrt{\beta(a)^2 - \log \mathfrak{R}'_u}$
 - (b) If, $\frac{a-z^*}{-z^*} > \mathfrak{R}''_u$ then return z^* , else go to step 2
 3. Else,
 - (a) Compute $z^* = \beta(a) + [a - \beta(a)]\mathfrak{R}'_u$
 - (b) If, $\frac{a-z^*}{a-z(a)} \exp(z(a)^2 - (z^*)^2) > \mathfrak{R}''_u$ then return z^* , else go to step 2
- If $a \geq 0$,
 1. If $\frac{1}{2a\sqrt{\pi} + 1} > \mathfrak{R}_u$ then $z^* = -\sqrt{-\log \mathfrak{R}'_u}$, else $z^* = \frac{1}{\sqrt{2}}\mathfrak{R}_u$
 2. If $\frac{a-z^*}{a} > \mathfrak{R}''_u$ then return z^*
 3. Else go to 1

Recommended generator for general problems.

For the velocity distribution, the y and z components are independent and generated as

$$v_y = V_y + \sqrt{\frac{1}{2}}v_T \mathfrak{R}_n, \quad v_z = V_z + \sqrt{\frac{1}{2}}v_T \mathfrak{R}'_n,$$

where $\mathfrak{R}_n, \mathfrak{R}'_n$ are independent, normal (Gaussian) distributed random values with zero mean and unit variance.

For the special case $V_x = 0$, the normal component is easily generated as

$$v_x = v_T \sqrt{-\log \mathfrak{R}_u},$$

where \mathfrak{R}_u is a uniformly distributed random value in the interval (0, 1). In the general case ($V_x \neq 0$), we generate this component as

$$v_x = (a - z^*)v_T = V_x - z^*v_T,$$

where z^* is generated from the Maxwell inflow distribution.

From our studies, we recommend generating z^* by the method outlined in Table 1 for the low-speed flows in the approximate range $-0.4v_T < V_x < 1.3v_T$ (see Figs. 3 and 4). This method uses Envelope 1 (Section 5.2.1)

Table 3

Outline of inversion method

1. Select the desired absolute error, E_d
2. Set $u = \mathfrak{R}_u$, $k = 0$, $m(a) = \exp(-a^2) + a\sqrt{\pi}[1 + \operatorname{erf}(a)]$
3. Compute initial guess $z_0 = \frac{1}{2}(a - \sqrt{a^2 + 2})$
4. Compute current absolute error, $E_k = \frac{1}{m(a)} \{ \exp(-z_k^2) + a\sqrt{\pi}[1 + \operatorname{erf}(z_k)] \}$
5. If $|E_k| < E_d$, then return $z^* = z_k$
6. Else,
 - (a) Compute new guess, $z_{k+1} = z_k - \frac{E_k m(a)}{2(a - z_k) \exp(-z_k^2)}$
 - (b) Set $k = k + 1$ and go to step 4

Table 4

Outline of box envelope method

1. Select $z_<(a)$ and $z_>(a)$. Typically $z_<(a) = \min(a - \alpha_1, -\alpha_2)$, $z_>(a) = \min(a, \alpha_2)$ with $\alpha_1 = 1$ or 2 and $\alpha_2 = 3$
2. Set $z(a) = \frac{1}{2}(a - \sqrt{a^2 + 2})$
3. Compute $z^* = z_<(a) + [z_>(a) - z_<(a)]\mathfrak{R}_u$
4. If $\frac{a - z^*}{a - z(a)} \exp(z(a)^2 - (z^*)^2) > \mathfrak{R}'_u$ then return z^* , else go to step 3

Table 5

Outline of reservoir envelope method

1. Select $z_<(a)$. Typically $z_<(a) = \min(a - 1, -\alpha_R)$ with $\alpha_R = 3$
2. If $a \leq 0$, compute $z^* = -\frac{1}{\sqrt{2}}|\mathfrak{R}_n|$, else $z^* = \frac{1}{\sqrt{2}}\mathfrak{R}_n$
3. If $\frac{a - z^*}{a - z_<(a)} > \mathfrak{R}_u$ then return z^* , else go to step 2

for $a \leq 0$ and Envelope 3 (Section 5.2.3) for $a > 0$. The method outlined in Table 2, which uses Envelope 2 (Section 5.2.2) for $a < 0$ and Envelope 4 (Section 5.2.4) for $a \geq 0$, is recommended for high speed or mixed speed flows. For reference, three alternative methods in common use, inversion (Section 4), box envelope (Section 5.1.1), and reservoir (Section 5.1.2), are outlined in Tables 3–5.

The various numerical schemes outlined in this paper are summarized in Tables 1–5. In those tables, \mathfrak{R}_u , \mathfrak{R}'_u , and \mathfrak{R}_u'' are independent, uniformly distributed random values in the interval (0, 1) and \mathfrak{R}_n is a normal (Gaussian) distributed random value with zero mean and unit variance.

8. Concluding remarks

To summarize the main results, two new formulations are developed for generating random values from the Maxwell inflow distribution (1.1). For small-speed ratio, approximately in the range $-0.4 < a < 1.3$, acceptance–rejection using the envelopes in Sections 5.2.1 and 5.2.3 is recommended. For the more general case, acceptance–rejection using the envelopes in Sections 5.2.2 and 5.2.4 are recommended. These new formulations are simple to implement (see Tables 1 and 2) and are several times faster computationally than the generators in common use (see Section 6).

The most common application for generators of the Maxwell inflow distribution is the implementation of open boundary conditions for particle simulations, especially direct simulation Monte Carlo (DSMC) and related schemes based on the Boltzmann equation [7]. Adaptive algorithm hybrids [11–13], which couple a particle simulation with a continuum solver, also generate random velocities for particles crossing the algorithms’ interface. Another numerical application is the computation of Master equation trajectories for Brownian systems, such as the “adiabatic piston” and thermal Brownian motors [14].

Finally, the Maxwell inflow distribution may be used in the construction of generators for other distributions. For example, [15] describes two iterative methods that use the simple Maxwellian (Gaussian) generator

to produce random values from the Chapman–Enskog distribution. It should be possible to generalize these methods to generate efficiently the Chapman–Enskog inflow distribution using the Maxwell inflow distribution schemes presented in this paper.

Appendix A. Inflow functionals and transformations

Let e be given in spherical coordinates as

$$e = (\cos \varphi \sin \theta, \sin \varphi \sin \theta, \cos \theta), \quad \varphi \in [0, 2\pi), \quad \theta \in [0, \pi].$$

Introduce the orthogonal matrix

$$Q(e) = \begin{pmatrix} \cos \varphi \cos \theta & -\sin \varphi & \cos \varphi \sin \theta \\ \sin \varphi \cos \theta & \cos \varphi & \sin \varphi \sin \theta \\ -\sin \theta & 0 & \cos \theta \end{pmatrix} \tag{A.1}$$

and note that

$$Q(e)'e = (0, 0, 1),$$

where Q' denotes the transposed matrix. Using the substitution

$$v = V + \sqrt{2T}Q(e)w, \quad dv = (2T)^{3/2}dw, \tag{A.2}$$

and taking into account that

$$(V + \sqrt{2T}Q(e)w, e) = (V, e) + \sqrt{2T}w_3 \tag{A.3}$$

and

$$M_{e,v,T}(V + \sqrt{2T}Q(e)w) = \frac{\rho}{(2\pi T)^{3/2}} \exp(-\|w\|^2), \tag{A.4}$$

one obtains

$$\int_{\mathcal{R}^3} h(v)q(v) dv = \frac{\rho\sqrt{2T}}{C\pi^{3/2}} \int_{\mathcal{R}^3} h(V + \sqrt{2T}Q(e)w) \exp(-\|w\|^2)(a + w_3)\chi(a + w_3) dw, \tag{A.5}$$

where h is any given function, q and a are defined in (2.5) and (3.1), respectively, and χ denotes the Heaviside function.

In particular, (A.5) allows us to calculate functionals of the normal velocity component of the incoming particles (cf. (2.5)), that is,

$$\Phi(\psi) = \int_{\mathcal{R}^3} \psi((v, e))q(v) dv. \tag{A.6}$$

Moments are obtained for

$$\psi(x) = \psi_k(x) = x^k, \quad k = 1, 2, \dots \tag{A.7}$$

These moments will quantify the errors in the approximate generators (see Section 5.1.3). One obtains from (A.5) that

$$\Phi(\psi) = \frac{\rho}{C} \sqrt{\frac{2T}{\pi}} \int_{-\infty}^a \psi(\sqrt{2T}(a - z))(a - z) \exp(-z^2) dz. \tag{A.8}$$

Note that

$$\int_{-\infty}^x \exp(-z^2) dz = \frac{\sqrt{\pi}}{2} [1 + \operatorname{erf}(x)] \quad \forall x \in \mathcal{R}, \tag{A.9}$$

$$\int_{-\infty}^x (-z) \exp(-z^2) dz = \frac{1}{2} \exp(-x^2) \quad \forall x \in \mathcal{R}, \tag{A.10}$$

and

$$\int_0^x z^2 \exp(-z^2) dz = \frac{\sqrt{\pi}}{4} \operatorname{erf}(x) - \frac{x}{2} \exp(-x^2) \quad \forall x \geq 0, \quad (\text{A.11})$$

where

$$\begin{aligned} \operatorname{erf}(y) &= \frac{2}{\sqrt{\pi}} \int_0^y \exp(-z^2) dz, \quad y \geq 0, \\ \operatorname{erf}(y) &= -\operatorname{erf}(-y), \quad y < 0. \end{aligned} \quad (\text{A.12})$$

Since $\Phi(1) = 1$ (cf. (A.6)), we obtain from (A.8) (cf. (2.4) and (3.2))

$$C = \varrho \sqrt{\frac{2T}{\pi}} \int_{-\infty}^a (a-z) \exp(-z^2) dz = \varrho \sqrt{\frac{T}{2\pi}} m(a). \quad (\text{A.13})$$

Thus, (A.8) takes the form

$$\Phi(\psi) = \frac{2}{m(a)} \int_{-\infty}^a \psi(\sqrt{2T}(a-z))(a-z) \exp(-z^2) dz. \quad (\text{A.14})$$

In particular (using (A.11)), one obtains the mean value (cf. (A.7))

$$\Phi(\psi_1) = \frac{2\sqrt{2T}}{m(a)} \int_{-\infty}^a (a-z)^2 \exp(-z^2) dz = \sqrt{\frac{T}{2}} \frac{\sqrt{\pi}[1 + \operatorname{erf}(a)](1 + 2a^2) + 2a \exp(-a^2)}{\sqrt{\pi}a[1 + \operatorname{erf}(a)] + \exp(-a^2)}.$$

References

- [1] L. Devroye, *Non-Uniform Random Variate Generation*, Springer, New York, 1986.
- [2] W. Hormann, J. Leydold, G. Derflinger, *Automatic Nonuniform Random Variate Generation*, Springer, New York, 2004.
- [3] J. Koplik, J.R. Banavar, *Ann. Rev. Fluid Mech.* 27 (1995) 257–292.
- [4] E.S. Oran, C.K. Oh, B.Z. Cybyk, *Ann. Rev. Fluid Mech.* 30 (1998) 403–441.
- [5] C.R. Lilley, M.N. Macrossan, *Int. J. Num. Meth. Fluids* 42 (2003) 1363.
- [6] C. Cercignani, *The Boltzmann Equation and its Applications*, Springer, New York, 1988.
- [7] G.A. Bird, *Molecular Gas Dynamics and the Direct Simulation of Gas Flows*, Clarendon Press, Oxford, 1994.
- [8] S. Rjasanow, W. Wagner, *Stochastic Numerics for the Boltzmann Equation*, Springer, Berlin, 2005.
- [9] M. Tysanner, A.L. Garcia, *Int. J. Num. Meth. Fluids* 48 (2005) 1337–1349.
- [10] W.H. Press, S.A. Teukolsky, Wm.T. Vetterling, B.P. Flannery, *Numerical Recipes in C++: The Art of Scientific Computing*, second ed., Cambridge University, Cambridge, 2002 (Section 6.2).
- [11] A. Garcia, J. Bell, Wm.Y. Crutchfield, B.J. Alder, *J. Comput. Phys.* 154 (1999) 134.
- [12] O. Aktas, N.R. Aluru, *J. Comput. Phys.* 178 (2002) 342.
- [13] P. Koumoutsakos, *Ann. Rev. Fluid Mech.* 37 (2005) 457–487.
- [14] P. Meurs, C. Van den Broeck, A.L. Garcia, *Phys. Rev. E* 70 (2004) 051109.
- [15] A.L. Garcia, B. Alder, *J. Comput. Phys.* 140 (1998) 66.
- [16] M. Matsumoto, T. Nishimura, *ACM Trans. Model. Comput. Simul.* 8 (1998) 3–30.